Journal of Korean Society of
Coastal and Ocean Engineers
Vol. 13, No. 1, pp. 80~87, March 2001

Robust Diagnostic World Ocean Circulation with Half-Degree Resolution
1/2° 解像度의 診斷的 全球 海水循環模型 硏究

Byung Ho Choi*, Zexun Wei*, Guohong Fang**, and Youngjin Choi*
최병호* · 웨이체첸* · 팡구오홍** · 최영진*

Abstract □ Global robust diagnostic models are established based on MOM of GFDL to study the circulation in the world ocean. The horizontal grid sizes 1/2 degree , and the vertical water column is divided into 21 levels. The hydrographic data are taken from Levitus *et al.*(1994) and the wind stress from Hellerman and Rosenstein (1983). Based on the model results the horizontal volume, heat and salt transports across some representative sections are calculated. The preliminary results show that: Though the cross-equator volume transports in the Atlantic, Indian and Pacific Oceans are all small, the heat transports across equator in the Atlantic are northward. This is clearly a result of the southward flow of the North Atlantic Deep Water and the northward compensating warm flow in the upper layer. The annual mean of the cross-equator heat transport in the Pacific Ocean from the present model is significantly lower than that calculated by Philander *et al.* (1987). This might indicate the importance of the Indonesian Throughflow in the heat transport in the Pacific Ocean. Our calculation shows that the heat transport through the Indonesian Archipelago is 0.5 PW, which is comparable with the poleward heat transport in the North Atlantic and Pacific Oceans. The difference in heat transports across the sections 5 and 6 demonstrates the important role of the Agulhas Current in the heat balance of the world ocean.
Keywords : diagnostic model, world ocean, North Pacific, circulation

要 旨 : GFDL의 진단적 모형인 MOM(Modular Ocean Model)을 이용한 전구 해수순환이 연구되었다. 모형의 수평 해상도는 1/2°이며, 수직으로는 21개의 층을 가지고 있다. 열염 관측자료로는 Levitus등(1994)의 자료를, 바람응력자료는 Hellerman과 Rosenstein(1983)의 자료를 사용하였다. 대표적인 분할지역을 가로지르는 수평적 유량 및 열염이송이 모형결과로부터 계산되었다. 초기결과로서 다음과 같은 사실을 알 수 있었다: 대서양, 인도양 및 태평양에서 적도를 통한 수송량이 매우 작았지만 적도를 횡단하는 대서양지역의 열수송은 관측결과에 의하면 북향이었는데 이는 명백히 상층의 난류를 보상하는 북대서양 심해에서의 남향 흐름의 영향이다. 본 연구에서 계산된 태평양 적도지역의 연평균 열수송량은 Philander등(1987)에 의해 계산된 값보다는 작은 값을 보였는데 태평양의 열수송에서 Indonesian Throughflow의 중요성을 말해주는 것으로 보인다. 본 연구에서는 인도네시안 군도를 통한 열수송량이 -0.5PW정도로 계산되었는데 북대서양과 태평양에서의 극방향 열수송과 비견될 만한 양이다. 구획5와 구획6해역의 열수송의 차이는 아굴라스 해류가 전구 해양의 열평형에서 차지하는 중요한 역할을 제시하였다.

핵심용어 : 진단적 모형, 전구 해양, 북태평양, 순환

1. INTRODUCTION

The rapid development of the computers has made it possible to simulate the ocean circulation using numerical modelsof three-dimensional primitive equations, especially for the large margin with fine resolution. GFDL (Geophysical Fluid Dynamic Laboratory)'s Modular Ocean Model (MOM) is one of this kind of models. It is based on Kirk

*Dept. of Civil and Environmental Engineering, Sung Kyun Kwan University, Suwon 440-746, Korea
**Dept. of Physical Oceanography, Institute of Oceanology, Chinese Academy of Sciences, 7 Nanhai Road, Qingdao 266071, China

Bryan(1969)'s work. As described by Bryan, the equations consist of the Navier-Stokes equations subject to the Boussinesq, hydrostatic, and rigid approximations along with a nonlinear equation of state which couples two active tracers, temperature and salinity to the fluid velocity. The diagnostic study on the world ocean circulation has been conducted by Fujio *et al.*(1991, 1992). The resolution of their model was 2°×2°, thus it was not able to resolve the marginal seas adequately. And their emphasis was on the water movement. Arakawa and Takano (1993) has also studied global ocean circulation but could not resolve mesoscale eddies as its coarse resolution of 2°×2°. And global eddy simulation has been applied by Semtner and Chervin (1988, 1992), but they did not resolve the East Marginal Seas (EAMS) adequately, because the coarse resolution and the model grid system are not suitable for resolving the EAMS. Semtner (1992) has reviewed the study of the global ocean circulation.

In the present study, we established a 1/2°×1/2° resolution robust diagnostic model for the world ocean based on MOM to study the circulation in the world ocean. Based on the model results, the horizontal volume, heat and salt transports across some representative sections are obtained.

2. MODEL DESCRIPTION

The governing equations are as follows:

$$\frac{\partial \boldsymbol{u}}{\partial t}+(\boldsymbol{u}\cdot\nabla)\boldsymbol{u}+w\frac{\partial \boldsymbol{u}}{\partial z}+f\boldsymbol{k}\times\boldsymbol{u}= -\frac{1}{\rho_0}\nabla p+A_H\nabla^2\boldsymbol{u}+A_v\frac{\partial^2\boldsymbol{u}}{\partial z^2}+minor\ terms \quad (1)$$

$$\frac{\partial p}{\partial z}+\rho g=0 \quad (2)$$

$$\nabla\cdot\boldsymbol{u}+\frac{\partial w}{\partial z}=0 \quad (3)$$

$$\frac{\partial \theta}{\partial t}+(\boldsymbol{u}\cdot\nabla)\theta+w\frac{\partial\theta}{\partial z}=K_H\nabla^2\theta+K_v\frac{\partial^2\theta}{\partial z^2}+\gamma(\theta^*-\theta) \quad (4)$$

$$\frac{\partial S}{\partial t}+(\boldsymbol{u}\cdot\nabla)S+w\frac{\partial S}{\partial z}=K_H\nabla^2 S+K_v\frac{\partial^2 S}{\partial z^2}+\gamma(S^*-S) \quad (5)$$

$$f=2\Omega\sin\phi \quad (6)$$

The damping terms $\gamma(\theta^*-\theta)$ and $\gamma(S^*-S)$ in the equations (4) and (5) were first proposed by Sarmiento and Bryan (1982), and the model was called *robust diagnostic* model. These terms force the model-produced temperature and salinity to approach the observed values.

Table 1. Depths and Thickness of Model Levels

Level	Depth range(m)	Thickness(m)	Mid-depth(m)
1	0~20	20	10
2	20~40	20	30
3	40~80	40	60
4	80~120	40	100
5	120~180	60	150
6	180~250	70	215
7	250~350	100	300
8	350~450	100	400
9	450~550	100	500
10	550~700	150	625
11	700~900	200	800
12	900~1100	200	1000
13	1100~1400	300	1250
14	1400~1750	350	1575
15	1750~2250	500	2000
16	2250~2750	500	2500
17	2750~3250	500	3000
18	3250~3750	500	3500
19	3750~4250	500	4000
20	4250~4750	500	4500
21	4750~5750	1000	5250

The horizontal resolution is 1/2 degree, and the vertical water column is divided into 21 levels (see Table 1). The domain is 0°-360°, 80°S-87°N. The topography is taken from DBDB5 data set (National Geophysical Data Center, Boulder, Colorado). The hydrographic data is taken from Levitus *et al.*(1994) and the wind stress from Hellerman and Rosenstein (1983).

The damping coefficient g was taken:

$$\gamma=[\gamma_d+(\gamma_0-\gamma_d)*e^{z/h}]*|\sin\varphi| \quad (7)$$

where γ_0 and γ_d are the surface and abyssal coefficients, set as $(100\ \text{day})^{-1}$ and $1/5\gamma_0$ respectively, z is the water depth, $h=500$ m, φ is the latitude. To restore the observed temperature and salinity quickly, we used larger γ during the first month integration.

As shown in Fujio *et al.* (1992), the diagnostic model is not significantly influenced by the choice of eddy mixing parameters. Thus we used the following values:

$A_H=1.0\times10^8$ cm^2/s, $A_v=1.0$ cm^2/s,
$K_H=1.0\times10^7$ cm^2/s, $K_v=0.2$ cm^2/s.

In the global model, we used the cyclic boundary condition on the east and west boundaries, and the solid boundary conditions on the north and south boundaries. We made 11-year integration forced by monthly steady hydrography and wind stress. The results of the last year were saved for analysis.

3. VOLUME, HEAT AND SALT TRANSPORTS

Model-produced transport stream functions are shown in Figs; 1(a) for annual mean, (b),(c),(d),(e) for seasonal mean of spring, summer, autumn and winter, respectively. From Fig. 1(a), we find that the basic pattern is quite similar to that of Fujio *et al.* (1992), except that some improvement can be seen. For example, the western boundary currents are strengthened and thus more realistic, and the Pacific equatorial counter current and the Mindanao dome have been better reproduced. These features were not resolved in Fujio *et al.* (1992) due to its coarse grid. From the Fig. 1(b)-(e), noticeable seasonal variations are also shown. The position of NEC (North Equatorial Current) is at the northernmost latitude in autumn and southernmost in spring. And some other detailed seasonal variations in the water, heat and salt transports are described subsequently.

To estimate the water volume, heat and salt transports in various regions we selected some representative sections in the oceans as shown in Fig. 2 and 3. The sections 1(C), 2(C) and 3(C) in the Pacific lie on the equator, 30°N and 30°S latitudes respectively. The transports across section 1(C) represent the energy and substance transfer between the North and South Pacific Ocean. The transport across the section 2(C) represent energy and substance transfer between the northern and southern North Pacific Ocean. In particular, the heat transports here characterize the poleward heat flux in the Pacific Ocean. The transports across the section 3(C) represent the energy and substance transfer between the Pacific and the Southern Oceans. The sections in the Atlantic and Indian Oceans are similar. The sections 4, 5 and 6 separate the southern Atlantic, Indian and Pacific Oceans, while section 7 passes through the Indonesian Archipelago. For short, the regions separated by these sections are named as in Fig. 2.

The sections 91~98 are representative sections in

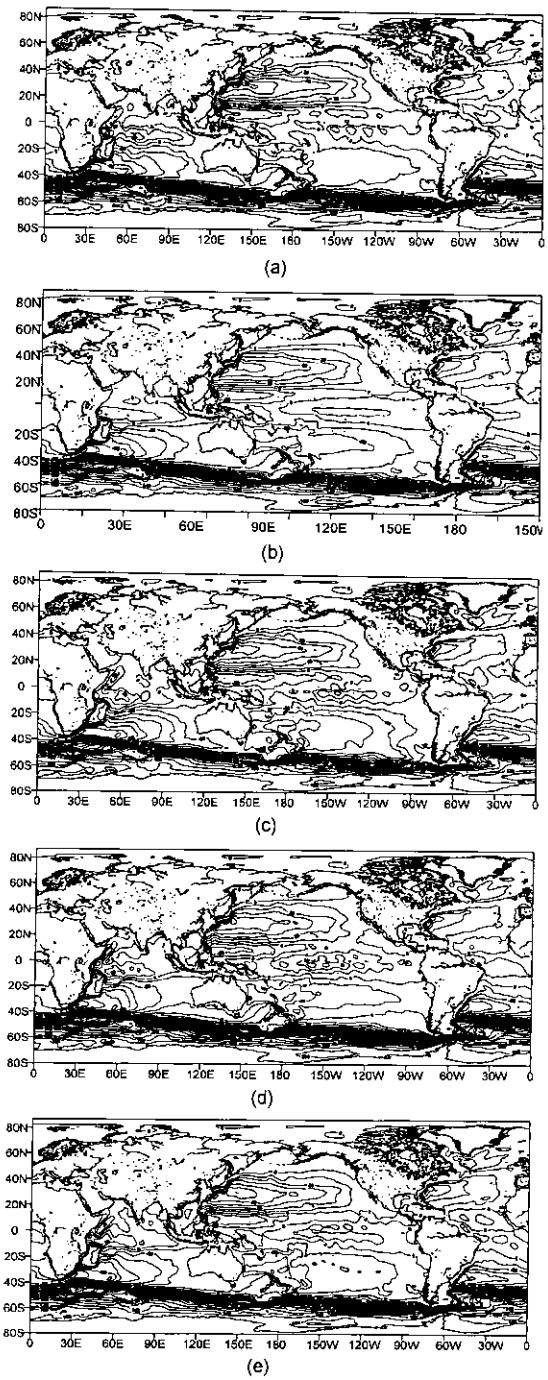

Fig. 1. (a) Transport stream function (unit:Sv) of the world ocean (annual mean), (b) Transport stream function (unit:Sv) of the world ocean (spring:MAM), (c) Transport stream function (unit:Sv) of the world ocean (summer:JJA), (d) Transport stream function (unit:Sv) of the world ocean (autumn:SON), (e) Transport stream function (unit:Sv) of the world ocean (winter:DJF).

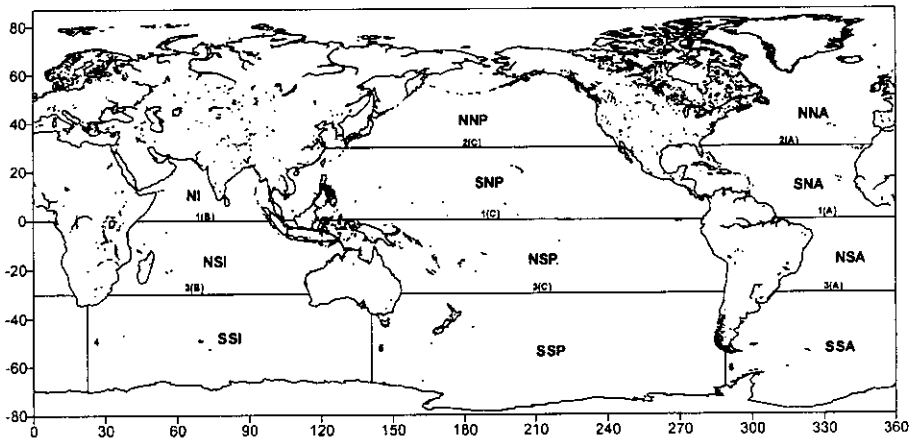

Fig. 2. The sections dividing the oceans into several regions.

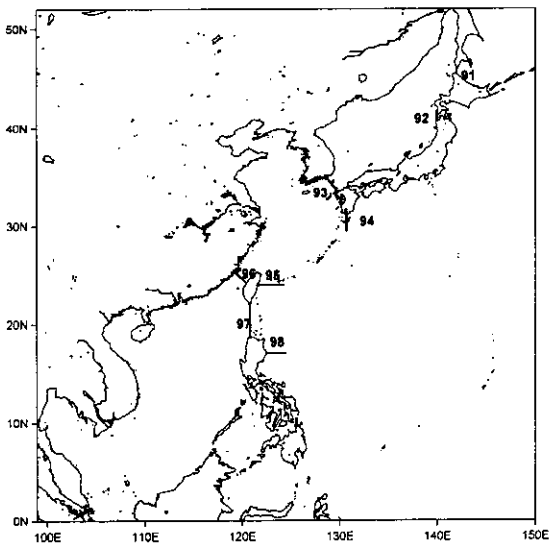

Fig. 3. The sections in East Asian marginal seas.

EAMS, which we have special attention to understand dynamics in the region. The sections 91, 92 and 93 lie on the Soya Strait, Tsugaru Strait and Korea Strait respectively. The sections 94, 95 and 96 lie on the south region of Kyushu, East of Taiwan Island and Taiwan Strait respectively. The section 97 and 98 lie on the Luzon (Bashi) Strait and the east region of Luzon Island, respectively.

Figures 4, 5 and 6 show the calculated water volume, heat and salt transports across the above representative sections. The unit is Sv ($1Sv = 10^6$ m^3/s) for the water volume transport, the unit for heat transport and salt transport are PW($1PW=10^{15}$ W) and Tg/s(Tera Grams/ sec.) respectively. All these transports are denoted as positive when they are eastward and northward, respectively.

3.1 Water Volume Transport

The model result shows that: the Antarctic Circumpolar Current (ACC) has a volume transport of 100-220 Sv from the southern South Indian Ocean (SSI) to the southern South Pacific (SSP), 80-200 Sv both from SSP to the southern South Atlantic (SSA) and from SSA to SSI. It indicates that there should be a pathway allowing the water to flow from the Pacific Ocean towards the Indian Ocean and then joining ACC and to return to the Pacific Ocean. By examining the transports across section 3(C), 7 and 3(B), we find that the transport from SSP to the northern South Pacific(NSP) is 4-18 Sv, the volume transport of the Indonesian Throughflow from the Pacific Ocean to the Indian Ocean varies from 0 to 18 Sv, and that from the northern South Indian Ocean(NSI) to SSI is 4-18 Sv. This shows that the water volume transport is almost in balance. A rate of 0-18Sv (with an average of 12Sv) for the Indonesian Throughflow is not very different with the simulated result of Godfrey(1989)(16 ± 4Sv.) and the observational result of Fieux *et al.*(1994) (18.6 ± 7Sv.).

Very small water flows across the equator in the Pacific, Atlantic and Indian Oceans, for that the northern boundaries of these oceans in the model are not connected to each other. For the EAMS, the water volume transport across east of Luzon Island is about 9-21 Sv. And then water is transported from the Pacific Ocean to the South China Sea

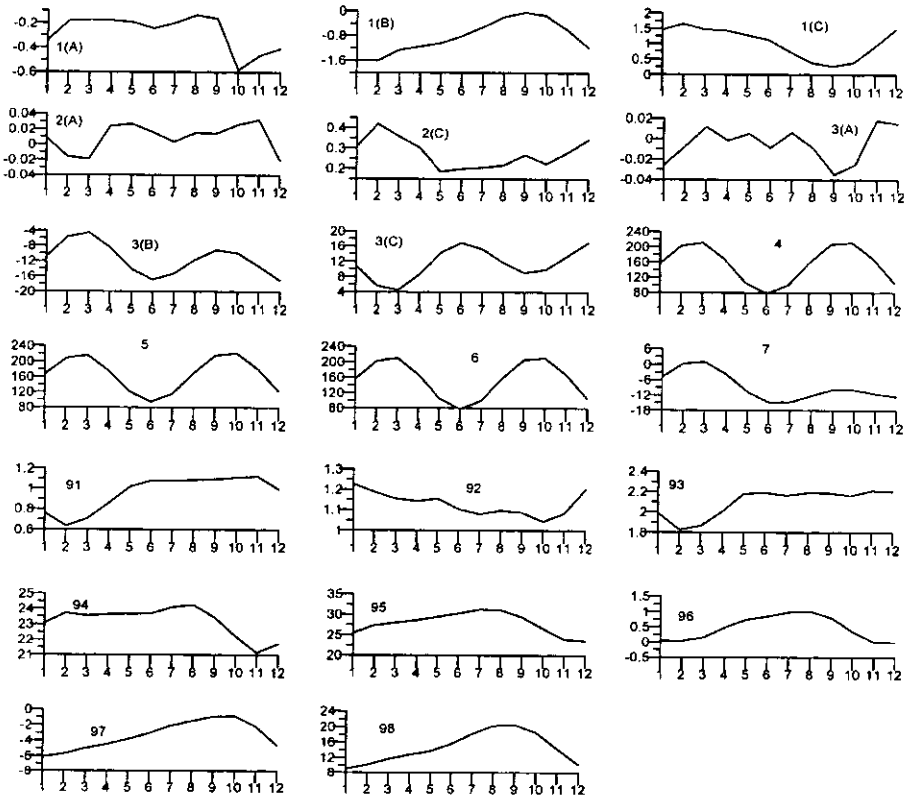

Fig. 4. The water volume transports (in Sv).

through the Luzon(Bashi) Strait at rates of 1-6 Sv, northward flows through the Taiwan Strait and the eastern region of the Taiwan Island are at 0.1-1.0Sv and 25-30Sv respectively. Water flows from the East China Sea to the Pacific through the north of Ryukyu Islands and to East/Japan Sea through Tsushima Strait are at 21-24.3Sv and 1.8-2.2Sv respectively. The volume transports from East/Japan Sea to the Pacific through the Tsugaru Strait and Soya Strait are about 0.6-1.1 Sv and 1.0-1.2Sv respectively.

3.2 Heat Transport

The heat transport across the equator in the Atlantic Ocean is from 0.3 to 1.0 PW, and that in the Indian Ocean is from −1.0 to 1.0 PW. The heat transport across the equator in the Pacific Ocean varies from −1.5 PW in summer to 1.7 PW in winter. This seasonal characteristics is in agreement with the result of Philander *et al.* (1987), who computed the seasonal variation of the zonally integrated meridional heat transport for the tropical Pacific Ocean. But our annual average of the cross-equator heat transport in the Pacific is lower than that calculated by Philander *et al.* (1987). This is most likely a consequence of the negligence of the Indonesian Throughflow in the Philanders model. Across the latitude 30°N, the heat transport in the Pacific Ocean varies from −0.2 to 1.2 PW with an average of 0.6 PW. The heat transport in the Atlantic at 30°N varies from 0.5 to 1.0 PW with an average of 0.7 PW. Yu and Malanotte-Rizzoli(1998) calculated the heat transports in the North Atlantic using an inverse model. The annual average at 25°N is 0.7 PW, quite close to our result. In spite of large volume transport of ACC, the eastward heat transports of section 4, 5 and 6 are not accordingly large. The reason is that the temperature near the Antarctica is very low. The heat transport across section 5 is about 0.5 PW more than that across section 6. It indicates that a certain amount of heat in the SSP is lost. Checking the heat transport across the section 3(C), we find that about 0.5 PW is transferred from the Southern Ocean to the Pacific Ocean. Across the

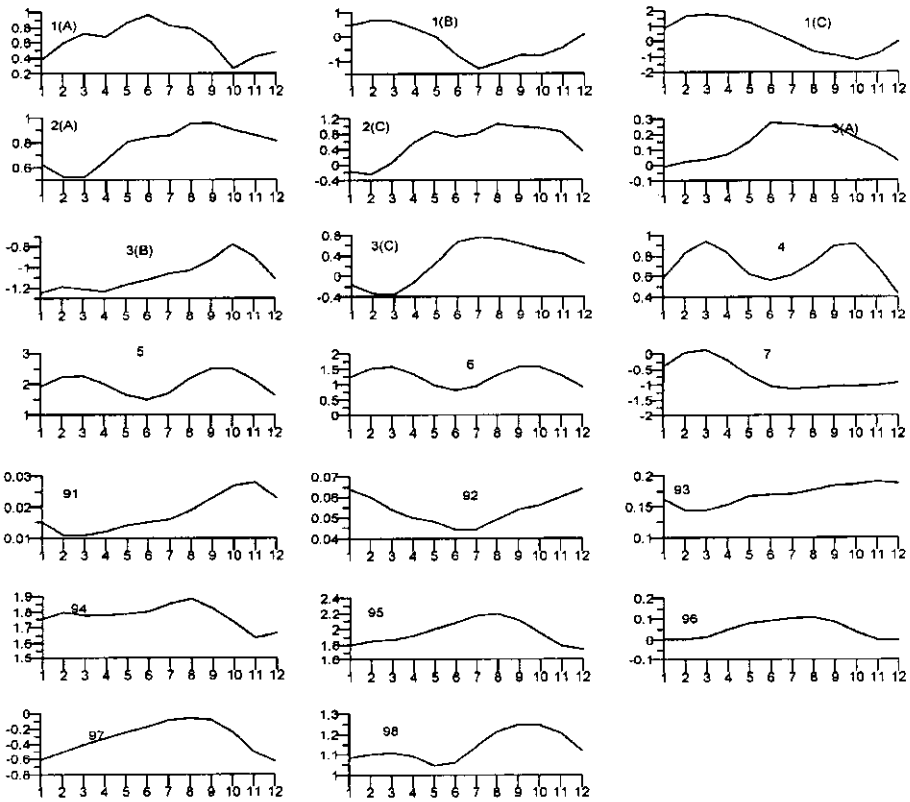

Fig. 5. The heat transport (in PW).

sections of 30°S, the heat transports in the Atlantic Ocean and Indian Ocean vary from 0.1(in winter) to 0.3(in summer) PW with an average of 0.15 PW and –0.8 to –1.2 PW with an average of –1.0 PW respectively. It means that across the latitude 30°S, the heat is transported northward in the Atlantic and Pacific Ocean, while southward in the Indian Ocean. These differences can be mainly attributed to the Agulhas Current and Indonesian Throughflow. The heat transport through the Indonesian Archipelago ranges from –1.0 PW to –0.1 PW, with the annual average of –0.5 PW.

In the EAMS, the simulated heat transports are: the heat transport across section 98 (East of Luzon Island) is about 1.0 to 1.2 PW, that across section 97 (Luzon Strait) is about –0.1 to –0.6 PW (that means the heat is transported into South China Sea), and that across Taiwan Strait (section 96), east of Taiwan Island are –0.0 –0.1 PW and 1.7 to 2.2 PW respectively. For the East/Japan Sea, the heat transports across the Korea Strait, Soya Strait and Tsugaru Strait are 0.14-0.18 PW, 0.01-0.03 PW and 0.042 to 0.065 PW respectively.

3.3 Salt Transport

The salt transports across the equator vary from 0.02 Tg/s (in summer) to 0.09 Tg/s (in winter) in the Pacific Ocean, from –0.02(in autumn) to 0.01 Tg/s (in summer) in the Atlantic Ocean, and from –0.05 (in winter) to 0.0 Tg/s(in autumn) in the Indian Ocean. Across the latitude 30°N, the salt transport in the Pacific Ocean is about 0.021 to 0.028 Tg/s with a small seasonal variation, and that in the Atlantic Ocean is from 0.004 to 0.015 Tg/s with a small seasonal variation too. Across the latitude 30°S, the salt transports are from –0.004 to –0.01 Tg/s in the Atlantic Ocean, from –0.1 to –0.6 Tg/s in the Indian Ocean, and from 0.18 to 0.6 Tg/s in the Pacific Ocean. For ACC, the eastward salt transports across section 4, 5 and 6 are very large. They are from 2.5 to 7.0 Tg/s (in summer) across section 4, from 3.5 to 8.0 Tg/s across section 5, and from 2.5 to 7.0 Tg/s across section 6. This seasonal variation denotes that the eastward salt transports

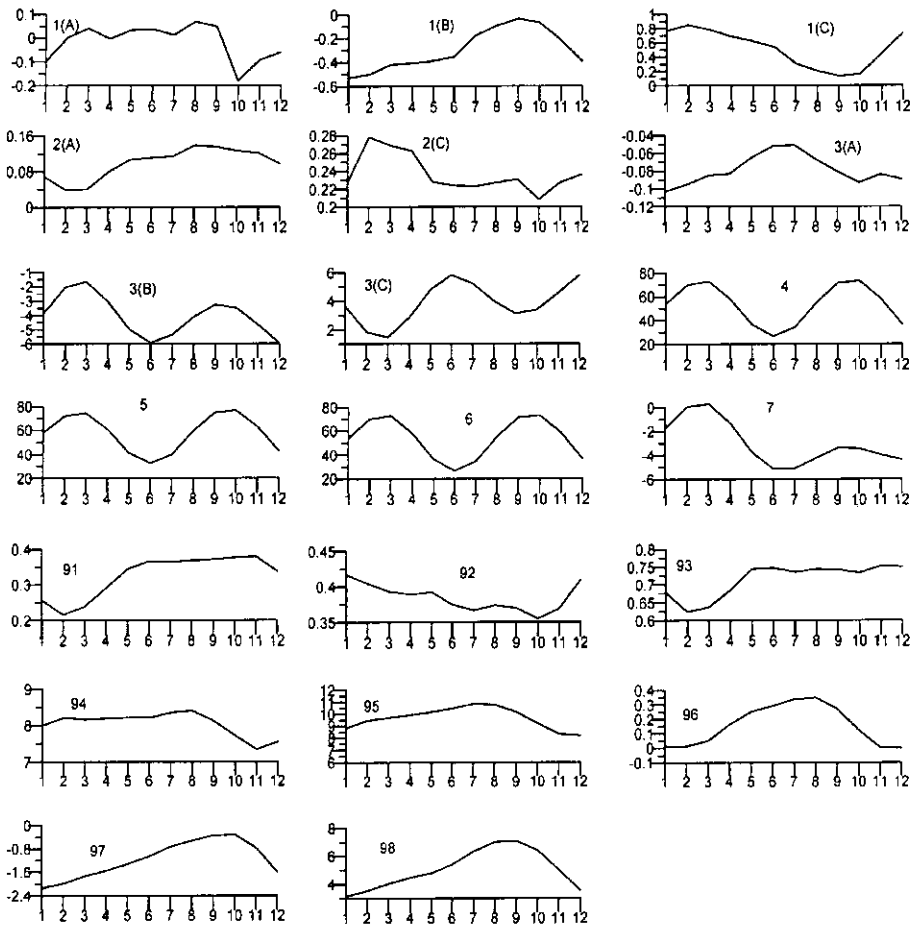

Fig. 6. The salt transports (in 10^{-1} Tg/s).

near the Antarctic are large in spring and autumn, small in winter and summer.

Due to the limited length of the present paper, we did not describe the salt transports in the EAMS in the present paper.

4. CONCLUDING REMARKS

The 1/2 degree diagnostic model of the present study can reasonably well reproduce the basic patterns of the general circulation in the world ocean. Though the cross-equator transports in the Atlantic, Indian and Pacific Oceans are all small, the heat transports across equator in the Atlantic is northward. This is clearly a result of the southward flow of the North Atlantic Deep Water and the northward compensative warm flow in the upper layer. The annual mean of the cross-equator heat transport in the Pacific from the present model is significantly lower than that calculated by Philander *et al.* (1987). This might indicate the importance of the Indonesian Throughflow in the heat transport in the Pacific. Our calculation shows that the heat transport through the Indonesian Archipelago is –0.5 PW, which is comparable with the poleward heat transport in the North Atlantic and Pacific Oceans. The difference in heat transports across the sections 5 and 6 demonstrates the important role of the Agulhas Current in the heat balance of the world ocean.

Nevertheless the present work did not reproduce some observational features, for example, the position of the Kuroshio deviates eastward. This is likely a result of the coarse resolution in the available climatological hydrographic data. To better simulate the western boundary

current diagnostically, a refined temperature and salinity climatological data set is required.

ACKNOWLEDGMENTS

The present work was supported by the National Science Foundation of China Grants 49576280 and 49876010, and by the Major State Basic Research Program, No. G1999043808. The work was also partially supported by Daewoo Corporation, Korea for the first author.

REFERENCES

Arakawa, C. And Takano, K., 1993. A numerical simulation of the general circulation in the world ocean, *La mer*, Part 1. Temperature and velocity fields, **31**, pp. 107-116.

Arakawa, C. And Takano, K., 1993. A numerical simulation of the general circulation in the world ocean, *La mer*, Part 2. Meridional and Interoceanic heat transport, **31**, pp. 117-124.

Bryan, K., 1969. A numerical method for the study of the circulation of the world ocean, *Journal of Computational Physics*, **4**, pp. 347-376.

Fujio, S. and Imasato, N., 1991. Diagnostic calculation for circulation and water mass movement in the deep Pacific, *J. Geophys. Res.*, **96**, pp.759-774.

Fujio, S. *et al.*, 1992. World ocean circulation diagnostically derived from hydrographic and wind stress fields, 1. The velocity field, *J. Geophys. Res.*, **97**, pp. 11163-11176

Fujio, S. *et al.*, 1992. World ocean circulation diagnostically derived from hydrographic and wind stress fields, 2. The water movement. *Res.*, **97**, pp. 14439-14452.

Fang, G. *et al.*, 1998. A survey of studies on the South China Sea upper ocean circulation. *Acta Oceanographica Taiwanica*, **37**(1), pp. 1-16.

Fang, G. *et al.*, 1991. Water transport through the Taiwan Strait and the East China Sea measured with current meters. *Oceanography of Asian Marginal Seas(Ed. K. Takano), Elsevier, Holland*, pp. 345-358.

Fieux, M. *et al.*, 1994. Measurements within the Pacific Indian oceans throughflow region, *Deep Sea Res., Part I.* **41**, pp. 1091-1130.

Godfrey, J. S., 1989. A Sverdrup model of the depth-integrated flow for the world ocean allowing for island circulations, *Geophys. Astrophys. Fluid Dyn.*, **45**, pp. 89-112.

Hellerman, S., Rosenstein, M., 1983. Normal monthly wind stress over the world ocen with error estimates, *Journal of Physical Oceanography*, **13**, pp. 1093-1104.

Levitus, S., 1982. Climatological atlas of the world ocean, *NOAA Prof. Pap. 13, 173pp*. U.S. Government Printing Office, Washington, D.C.

Philander, S., Hurlin, W.J., Seigel, A.D., 1987. Simulation of the seasonal cycle of the tropical Pacific ocean, *Journal of Physical Oceanography*, **17**, pp. 1986-2002.

Sarmiento, J. L., and K. Bryan, 1982. An ocean transport model for the North Atlantic, *J. Geophys. Res.*, **87**, pp. 394-408.

Semtner, A.J., R. M. Chervin, 1988. A simulation of the global ocean circulation with resolved eddies, *J. Geophys. Res.*, **93**, 15502-15522.

Semtner, A.J., Jr., and R. M. Chervin, 1992. Ocean general circulation from a global eddy-resolving model, *J. Geophys. Res.*, **97**, 5493-5550.

Yu, L. and P. Malanotte-Rizzoli, 1998. Inverse modeling of seasonal variations in the North Atlantic Ocean, *J. Phys. Oceanogr.*, **28**, 902-922.